

Change of fuel-to-cladding gap width with the burn-up in FBR MOX fuel irradiated to high burn-up

Koji Maeda^{*}, Takeo Asaga

Fuels and Materials Division, O-arai Engineering Center, Japan Nuclear Cycle Development Institute, 4002 Narita, O-arai-machi, Ibaraki 311-1393, Japan

Received 2 September 2002; accepted 6 January 2004

Abstract

In order to study the dependence of the gap width change on the burn-up, the fuel-to-cladding gap widths were investigated by ceramography in a large number of FBR MOX fuel pins irradiated to high burn-up. The dependence of gap widths on the burn-up was closely connected with the formations of JOG (joint oxyde-gaine) and rim structure. The gap widths decreased gradually due to the fuel swelling until ~ 30 GWd/t, but beyond this burn-up the dependence showed two different tendencies. With the increase of burn-up, the gap widths decreased due to the increase of fuel swelling in the low fuel temperature region where the rim structure was observed, but they increased in the high fuel temperature region where the JOG rich in Cs and Mo formed in the gap.

© 2004 Elsevier B.V. All rights reserved.

PACS: 28.41.Bm

1. Introduction

The temperature distribution in fuel under the steady state operating condition is one of the most basic parameters to determine the stored energy and analyze the fuel performance in a reactor. Heat conductance across the fuel-to-cladding gap strongly affects this temperature distribution. According to one model developed so far [1], the wider gap lowers the heat conduction across the gap and results in the increase of fuel temperature, and conversely, narrowing or closing the gap leads to the decrease of fuel temperature. Then, knowledge on the burn-up dependence of the gap width is a basic necessity for the design and performance analysis of fuel pins.

Fuel center temperature in FBR fuel pins is high due to the high linear heat rating and sodium coolant temperature, in comparison with that in LWRs. Observations of FBR fuel pins showed that volatile fission products generated in the central region of fuel pellets such as I and Cs migrate axially to the lower temperature region in the fuel-to-cladding gap after radial migration in the fuel matrix [2,3]. This migration results in a mixture of compounds formed from fission products at high burn-up. The mixture of compounds is called JOG (joint oxyde-gaine) which defined as the solid medium located between the pellet and the cladding [4]. On the other hand, in the lower temperature region, most volatile fission products do not easily migrate and re-crystallization has been found in the rim region of fuel pellets [5] at high burn-up.

In this paper, the gap width change was investigated as a function of burn-up in a large number of FBR mixed oxide (MOX) fuel pins irradiated to high burn-up in the Japanese fast reactor 'JOYO'. The results were discussed in the context of formations of JOG and rim structure.

^{*} Corresponding author. Tel.: +81-29 267 4141x5514; fax: +81-29 267 7130.

E-mail address: k-mae@oec.jnc.go.jp (K. Maeda).

2. Experimental procedures

2.1. Fuel specimens and irradiation conditions

The content of PuO₂ in the MOX fuel was approximately 30 wt%. MOX fuel pellets were fabricated by conventional powder metallurgy, and were inserted into the stainless steel cladding of 20% cold worked SUS316. The fissile column length was 550 mm. After wires were spirally wrapped around the fuel pins, they were assembled in a hexagonal arrangement and then irradiated under the steady state operating condition in 'JOYO'. After the non-destructive post-irradiation examination (PIE) of fuel pins, such as gamma scanning and profilometry, 1–5 fuel pins of each assembly were supplied for destructive PIE.

Table 1 shows typical characteristics of fuel pins and the axial positions where the cross sections of specimens were examined, together with the irradiation conditions. The axial positions are expressed using mm/dfb which means the axial distance from the bottom of fissile column. The maximum burn-ups were 98 GWd/t in the assembly, 127 GWd/t in the fuel pin and 130 GWd/t in the specimen. Linear heat rating (LHR) of specimens ranged from 12.9 to 48.4 kW/m.

2.2. Examinations

More than three segments were sectioned from each fuel pin. Those segments were vacuum impregnated with epoxy resin and cut transversely into discs of about 5 mm thickness. These specimen cross sections were glued to epoxy stubs, and then ground and mirror-polished.

The fuel cross sections were mainly examined using optical microscopy (OM). The gap width and fuel swelling were evaluated from the observed results by the method described in the next section. The whole area occupied by a fuel pellet on the cross section of a fuel pin was also analyzed on an optical micrograph by an imaging method in order to evaluate fuel-to-cladding gap width change and fuel swelling. Some specimens were, moreover, examined by scanning electron microscope (SEM) and electron probe micro-analyzer (EPMA). The microstructure change occurred in the pellet periphery was observed by SEM and typical elements of the inclusions in the gap were identified by EPMA.

3. Results and discussion

3.1. Microscopic examination of fuel

Fig. 1 shows ceramographs for 5 as-polished cross sections of a fuel pin (G357) which was irradiated to the average burn-up of 110 GWd/t. The axial positions, LHRs and burn-ups are shown in Table 1. Fig. 1 shows that a large central void was formed in the cross section

of the fuel pin at the mid-position, 278.3 mm/dfb. Gaps appeared in the cross sections at positions above 48.4 mm/dfb, but the gap was almost closed in the cross section at 40.7 mm/dfb.

Fig. 2 shows an enlarged ceramograph on the cross section at the mid-position, 278.3 mm/dfb. The gap widths and the amount of inclusions in the gaps were not uniform and depended on the radial directions of the fuel periphery. That is, the gap widths and amount of inclusions were large in one radial direction, but were small in another. Also, some of the gaps were completely filled, but others were only partially filled, with inclusions. Similar phenomena were observed in gaps at axial positions above 48 mm/dfb. Figs. 3 and 4 show secondary electron images and electron microprobe element images obtained for typical gaps at the positions 278.3 and 527.5 mm/dfb. Inclusions rich in Cs and Mo were formed in the gaps. The evolution of inclusions in the gap is referred to as JOG (joint oxyde-gaine) [4].

Fig. 5(a) shows the microstructural change characteristic of the pellet periphery observed at the position of 41 mm/dfb. In addition, a SEM-fractograph (Fig. 5(b)) was obtained in the region adjacent to that where the microstructure was observed. The microstructure distance from the outer surface of the pellet ranged from 0 to 50 μm. Similarly to LWR fuel, the rim structure [5] could be seen. That is, the sub-divided grain structure of ~2 μm around pores developed from the as-fabricated grain structure, together with small sized intra-granular bubbles.

3.2. Gap width change

As no fuel-to-cladding gap width for any radial direction is representative in an observed cross section, an average gap width was determined from the area of the cross section within the cladding inner diameter, S_c and that of the fuel pellet cross section including cracks, S_f . The radial gap width, G_w was derived as follows:

$$G_w = \sqrt{S_c/\pi} - \sqrt{S_f/\pi}. \quad (1)$$

From the measured gap width, the degree of gap width change, η , was given by the following expression:

$$\eta = (G_{w_t} - G_{w_0})/G_{w_0}, \quad (2)$$

where G_{w_0} and G_{w_t} are the gap widths before and after the irradiation. The degree of gap closure $\eta = -1$ means closure of the gap, and $\eta = 1$ means a doubled gap width from the original value.

The gap widths on all cross sections of irradiated fuel pins listed in Table 1 were measured in order to investigate the gap width change as a function of burn-up. Fig. 6 shows the degree of the gap width change as a function of burn-up. In this figure, the axial length of the fissile column is divided into three regions in order to

Table 1
Major specifications and irradiation conditions of fuel pins

Pin ID	Fuel density (% TD)	Fuel diameter (mm)	Gap width (μm)	Pin average LHR (BOL ^a) (kW/m)	Pin average burn-up (GWd/t)	Axial position of cross section (mm/dfb ^b)	Local burn-up (GWd/t)	Local LHR (BOL ^a) (kW/m)
6364	93	4.63	160	26.1	4.6	29.7	3.8	21.9
						256.9	5.4	31.2
						419.7	4.4	25.4
70A6	93	4.63	160	30.4	13.6	218.9	11.2	25.0
						148.1	16.0	36.2
						434.5	12.5	28.0
						535.7	8.6	19.1
8152	93	4.63	160	31.6	31.4	28.6	25.9	26.1
						250.8	37.1	37.8
						421.9	30.4	30.3
						521.4	21.5	21.0
9160	93	4.63	160	25.5	45.9	24.2	39.6	22.3
						22.5	53.7	30.5
						435.1	42.5	22.7
						539.6	28.8	14.9
A060	93	4.63	160	30.9	49.4	25.9	40.2	24.8
						255.8	57.8	36.6
						535.7	33.0	20.3
C860	93	4.63	160	26.4	67.6	24.8	58.1	22.2
						135.9	71.7	28.1
						245.3	78.5	31.1
						394.9	69.4	27.2
						550.0	41.4	15.3
C7A6	94	4.63	160	24.8	58.9	25.3	51.2	21.1
						138.1	62.7	26.3
						250.3	68.4	29.0
						394.9	60.3	25.7
						545.6	37.3	15.9
D860	94	4.63	160	21.9	46.8	23.1	39.7	18.9
						140.3	50.1	23.9
						248.1	54.5	25.9
						394.9	48.2	22.2
						550.0	28.5	12.1
E2B3	94	4.63	160	26.1	63.8	247.5	53.2	21.8
						238.2	74.2	30.9
						545.6	40.7	15.5
E963	94	4.63	160	32.6	55.4	24.2	45.5	25.4
						249.7	64.2	38.6
						412.0	55.7	32.9
						548.4	36.7	20.0
E964	94	4.63	160	32.6	55.3	15.4	44.2	24.7
						239.3	63.9	38.5
						540.1	37.8	20.8
E359	93	4.63	160	32.0	68.8	22.6	57.6	26.5
						141.9	72.9	34.2
						276.1	80.0	37.7
						412.0	68.8	31.8
						547.3	45.2	20.1

(continued on next page)

Table 1 (continued)

Pin ID	Fuel density (% TD)	Fuel diameter (mm)	Gap width (μm)	Pin average LHR (BOL ^a) (kW/m)	Pin average burn-up (GWd/t)	Axial position of cross section (mm/dfb ^b)	Local burn-up (GWd/t)	Local LHR (BOL ^a) (kW/m)
98B4	85	5.40	190	41.1	36.0	280.0	42.2	48.4
						546.2	22.1	24.8
A102	93	5.40	190	31.1	54.2	275.0	62.5	36.3
						419.1	52.6	30.1
						547.8	35.3	19.7
A104	93	5.40	190	30.5	53.2	302.0	60.6	35.1
						419.1	51.7	29.6
						547.8	33.7	18.6
A429	85	5.40	190	30.1	54.7	13.2	44.7	24.2
						249.2	63.8	35.5
						547.8	33.8	18.0
H710	85	5.40	190	83.1	21.9	10.1	70.2	24.8
						69.9	78.5	27.1
						124.8	86.5	29.7
						250.9	95.5	33.0
						540.1	56.4	19.6
G305	85	5.40	190	25.3	98.8	40.2	88.4	22.3
						278.3	113.6	29.5
						528.0	69.7	17.6
G357	85	5.40	190	28.9	110.6	40.7	97.8	25.1
						48.4	99.5	25.6
						79.8	106.1	27.4
						278.3	127.0	33.8
						527.5	78.4	19.9
G311	85	5.40	190	25.8	100.6	100.2	100.6	25.6
						213.0	114.6	29.7
						353.9	109.9	28.5
						548.5	65.0	16.3
G331	85	5.40	190	27.1	105.0	48.5	94.1	24.0
						17.0	116.2	30.1
						210.9	119.8	31.2
						245.8	121.2	31.6
						287.8	120.8	31.6
						336.8	117.2	30.6
						391.0	109.3	28.3
						432.5	100.5	25.9
						448.5	96.2	24.8
						465.1	91.8	23.6
						G339	85	5.40
169.2	117.7	30.5						
210.6	121.4	31.7						
245.3	122.8	32.2						
287.6	122.5	32.1						
335.6	119.0	31.1						
391.1	110.8	28.8						
431.0	102.3	26.5						
445.9	98.2	25.4						
466.1	92.7	23.9						

^a Beginning of life.^b Distance from bottom of fissile column.

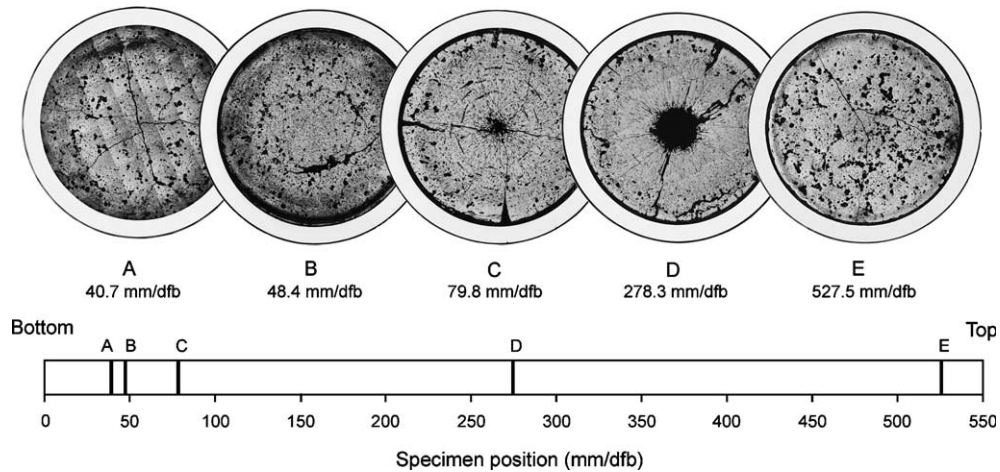


Fig. 1. Ceramographs of typical transverse sections in a high burn-up fuel pin (G357, Initial fuel density: 85% TD, pin average burn-up: 110.6 GWd/t).

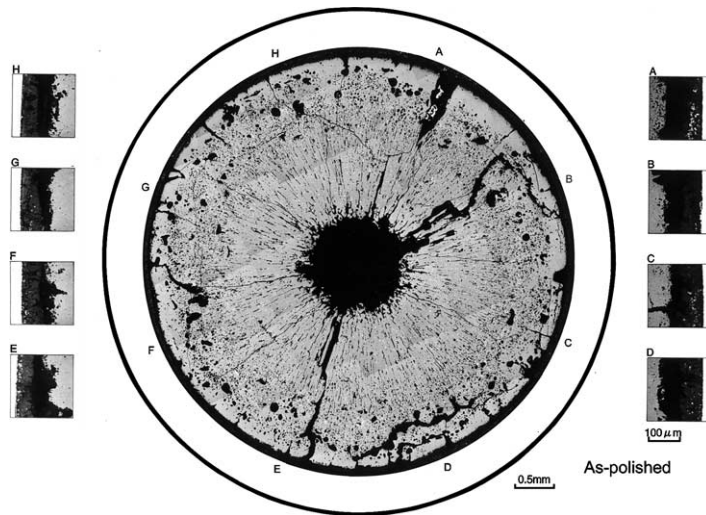


Fig. 2. Ceramograph of a transverse section and enlarged views of typical gap areas (G357, 278.3 mm/dfb).

classify the data. The boundaries between the lower and middle regions and between the middle and upper regions are located at the axial positions of 247.5 and 467.5 mm/dfb, respectively. The gap width described until ~ 30 GWd/t with the increase of burn-up. Beyond this burn-up, however, the dependence of gap width on the burn-up was of two types. The data in one types continued to decrease with increasing burn-up to 100 GWd/t and the data of the other type increased with increasing burn-up.

3.3. Gamma scanning

In order to investigate the axial migration of Cs, gamma scanning was carried out along the axial direction

of fissile column in fuel pins. Typical gamma scanning results for the G357 fuel pin are shown in Fig. 7. The bold line shows the amount of Cs calculated by the ORIGEN-2 code. Results indicated that Cs which was generated in the middle region of high temperature migrated to both upper and lower regions of low temperature. In addition, a sharp boundary could be seen just on the lowest position of the largest ^{137}Cs peak in the lower column region. This suggested that the gap was closed and the rim structure appeared below this boundary.

3.4. Fuel swelling

Fuel swelling was defined as the relative volume change. If the cross sections including the cracks within

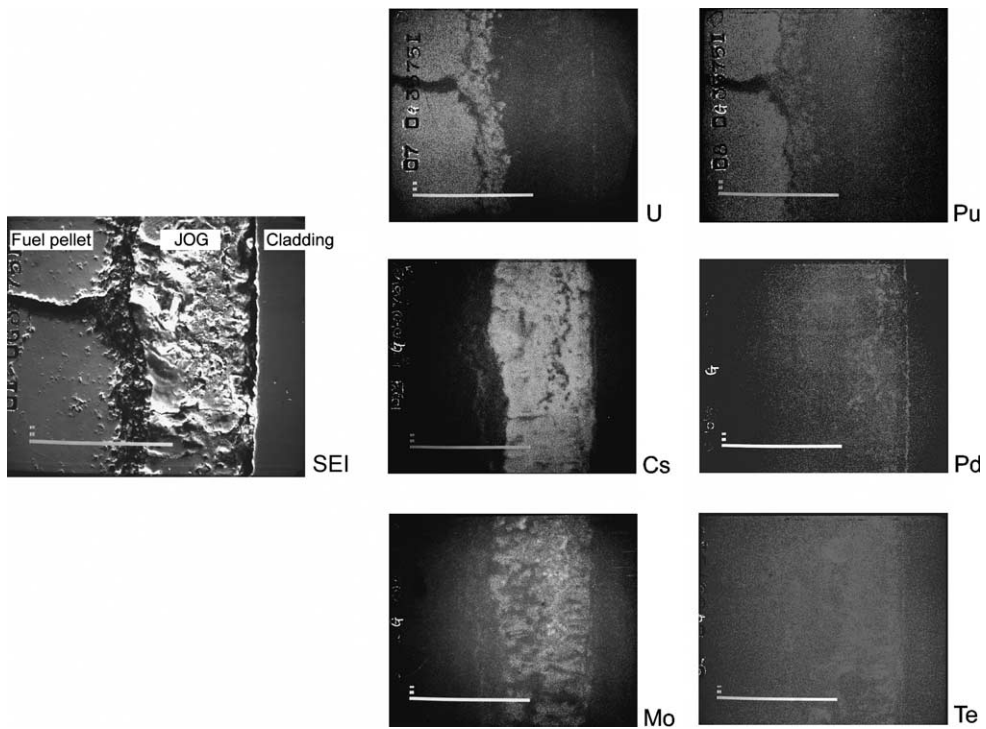


Fig. 3. X-ray image analysis of a fuel-to-cladding gap (G357, 278.3 mm/dfb).

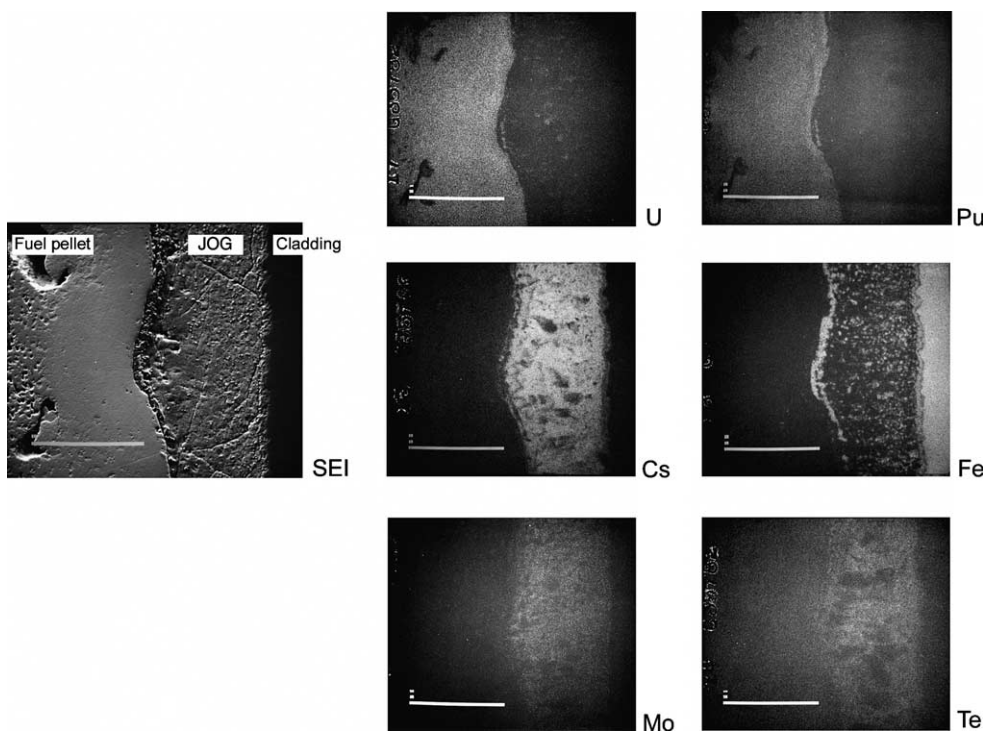


Fig. 4. X-ray image analysis of a fuel-to-cladding gap (G357, 527.5 mm/dfb).

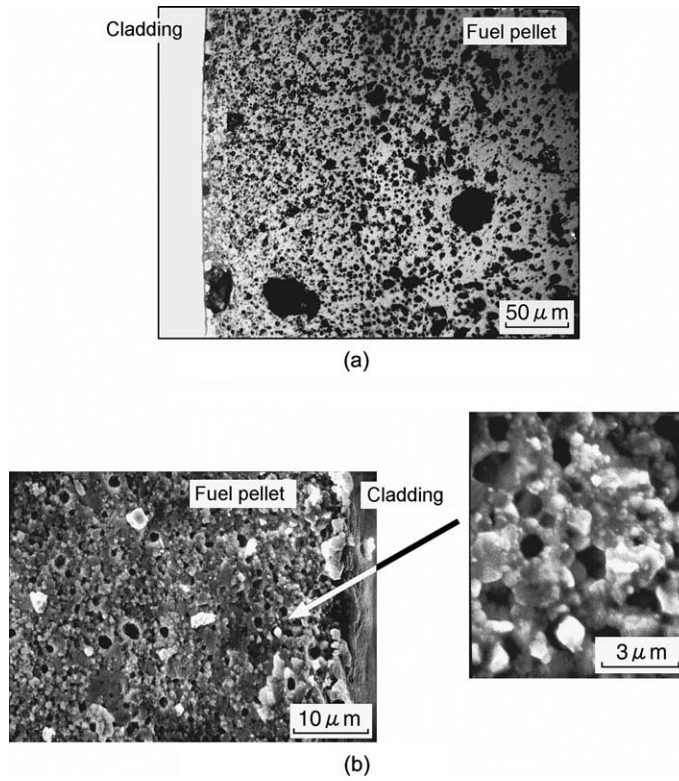


Fig. 5. Microstructure at pellet periphery (G357). (a) As-polished surface 40.7 mm/dfb (OM) and (b) fracture surface (SEM).

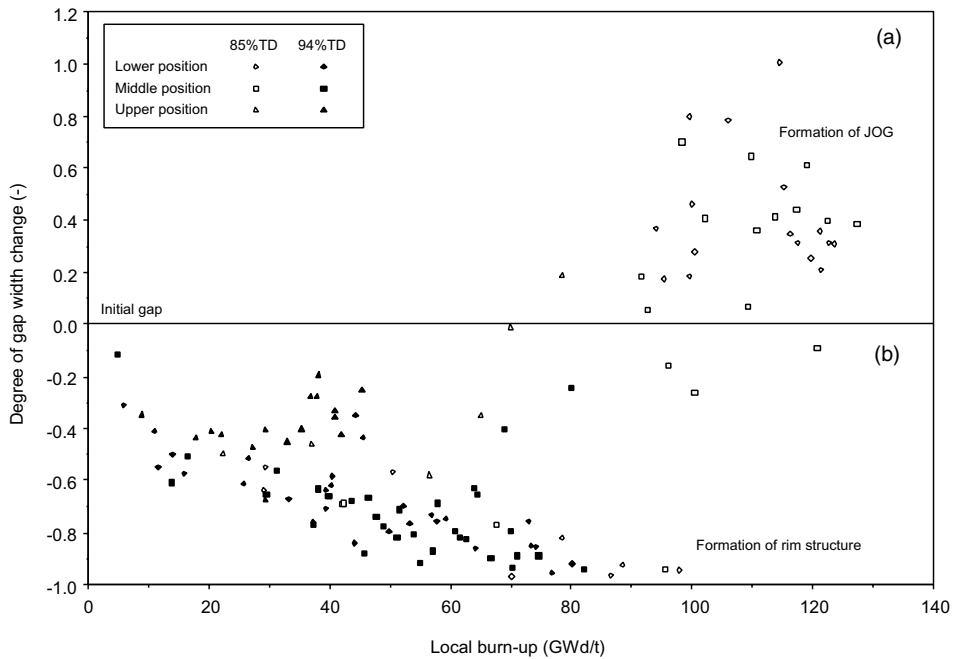


Fig. 6. Change in fuel-to-cladding gap width as a function of burn-up.

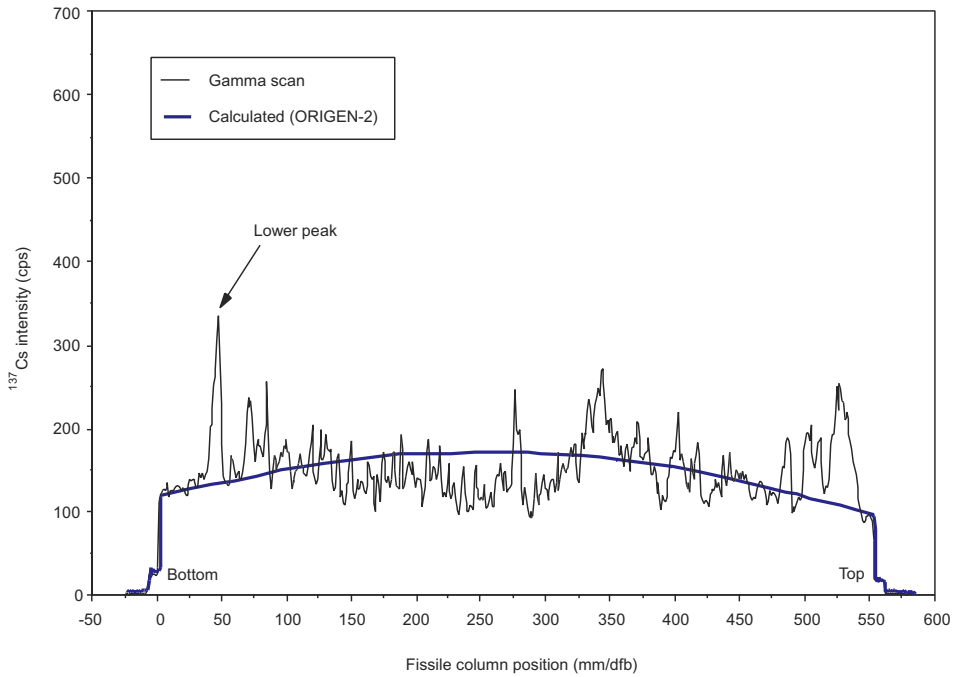


Fig. 7. Axial ¹³⁷Cs distribution along fissile column (G357).

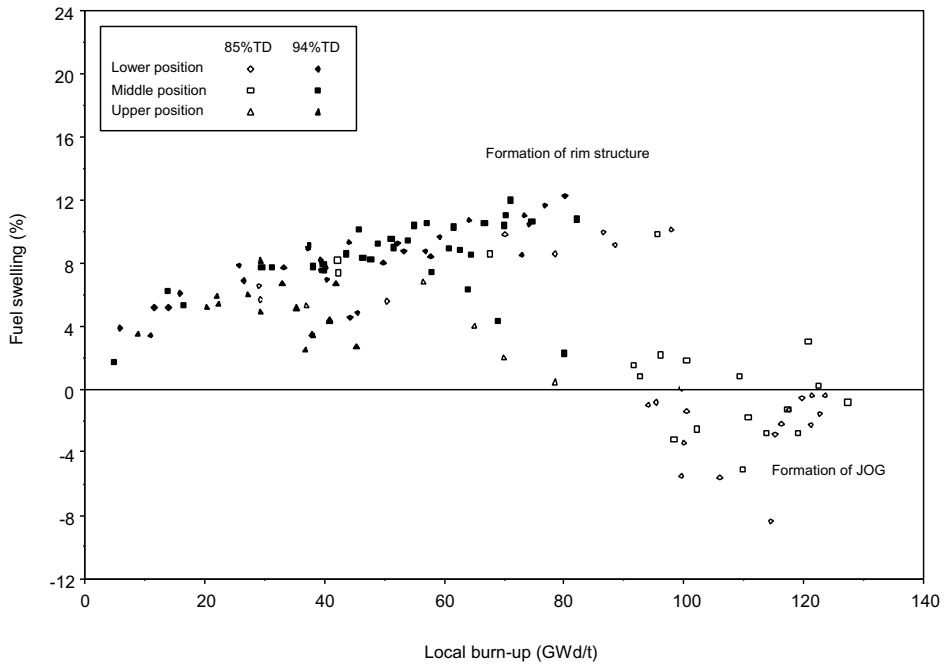


Fig. 8. Change in fuel swelling as a function of burn-up.

the fuel outer diameter of fuel before and after irradiation were, Sp and Sp' , respectively, the fuel swelling, $\nabla V/V$, was given as follows:

$$\frac{\nabla V}{V} = \frac{3}{2} \frac{(Sp' - Sp)}{Sp}. \quad (3)$$

Fig. 8 shows the fuel swelling on all cross sections examined as a function of burn-up. The fuel swelling increased with the burn-up due to accumulation of fission products and the occurrence of cracks in the fuel until the burn-up reached to ~ 30 GWd/t. When the burn-up exceeded this, the fuel swelling showed different tendencies, depending on the fuel specimens. The fuel swelling increased in some specimens, but decreased in others with the increase of burn-up.

4. Discussion

The decrease of the gap width with the increase of burn-up below ~ 30 GWd/t can be easily understood from the fact that the fuel swelling takes place due to the accumulation of gaseous and solid fission products in the fuel matrix. It should be noted in Fig. 7 that the irradiation-induced densification generally observed in LWR fuel cannot be seen below ~ 30 GWd/t. From a number of previous studies on densification, it is well known that small sized pores of less than ~ 2 μm in diameter in the as-fabricated fuel pellet have the most important effect on the densification, because the vacancies migrate to the grain boundary after solution from the pore to the fuel matrix by the fission fragments, and then the pores are annihilated. In this study, the fuel pellets were sintered at temperatures higher than 1700 $^{\circ}\text{C}$ with additive doping to form large pores in the pellet. It is reasonable to assume that the small fraction of pores less than ~ 2 μm in diameter made the irradiation-induced densification negligible.

As described already, the dependence of gap width and fuel swelling on the burn-up shows two different behaviors. In the lower and middle regions of fissile column where the fuel temperature is low, the gap width decreases and fuel swelling increases with the increase of burn-up. In addition, the re-crystallized structure known as the rim structure begins to develop in the rim region of fuel. It is, therefore, suggested that inter-granular bubbles due to the increases of fission gases and volatile fission products interconnect at grain edges, because they cannot easily move in low fuel temperature region (below 1000 $^{\circ}\text{C}$). The fission products precipitate in this region and cause pellet matrix swelling and rim bubble swelling.

On the other hand, the gap width continues to increase and the fuel swelling decreases together with the progressive formation of JOG beyond ~ 30 GWd/t in

the axial region of the fuel pin where the fuel temperature is high. This behavior can be explained as follows.

The fission gases and volatile fission products such as Cs and I of large ionic radii which are generated in the fuel matrix diffuse to, and accumulate in, the grain boundary below ~ 30 GWd/t. When the burn-up exceeds ~ 30 GWd/t, the volatile fission products migrate from the fuel matrix to the gap along the temperature gradient and subsequently form the JOG as shown in Figs. 3 and 4, because there is little capacity in the fuel matrix to accumulate additional fission products.

A part of the volatile fission products precipitated in the gap move axially to the low temperature region by the vaporization–condensation mechanism, as seen from ^{137}Cs redistribution in the gamma ray scanning curve along the fuel column shown in Fig. 7.

The increase of gap width by the formation of JOG raises the fuel temperature, although the extent of the temperature increase is lower when the gap is filled with only the fission gases instead of JOG [6–9]. This temperature increase accelerates the release of volatile fission products from the fuel matrix, resulting in the decrease of fuel swelling.

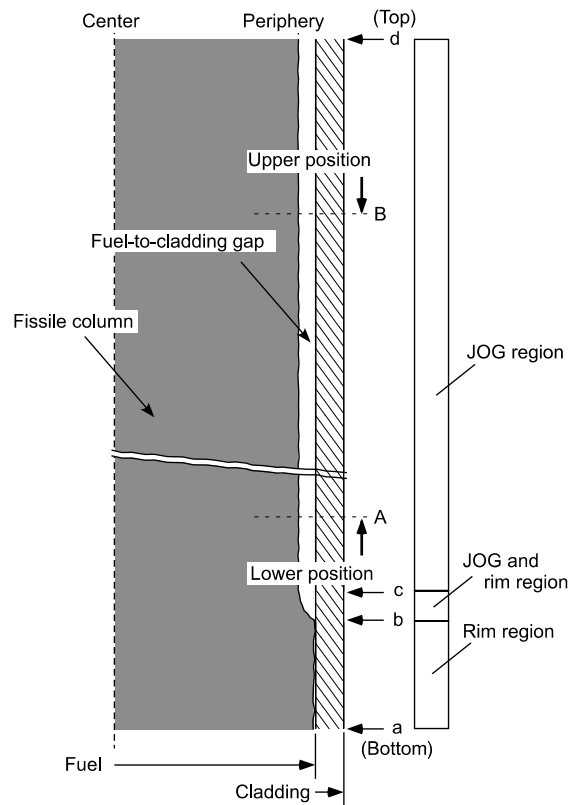


Fig. 9. Schematic diagram of gap width along the axial direction of fissile column.

Interesting behavior can be seen in Fig. 1 (picture B), which was obtained on the cross section at axial position, 48.4 mm/dfb. The gap is wide open in one radial direction, but closed in the opposite radial direction where the fuel pellet is expected to make contact with the inner surface of the cladding during irradiation. In the wide open gap, a large amount of volatile fission products accumulates, leading to the sharp peak of ^{137}Cs . However, rim structure develops to only a small extent in the fuel region where the gap closes.

The results on the gap width change are summarized in Fig. 9 as the dependence of gap width on the axial position. A and B are the boundaries between the lower and middle regions and between the middle and upper regions. Rim structure is formed in the axial region a–b where the fuel temperature is low, while JOG is formed in the region c–d where the fuel temperature is high. Both the rim structure and JOG coexist in the region b–c where the fuel temperature is intermediate.

The fuel temperature depends on the LHR, gap width and thermal conductivity of fuel. The thermal conductivity decreases with the decrease of initial fuel density. The axial position of the region b–c depends on the axial temperature distribution of the fuel pin. A higher LHR, larger gap width (Gw_0) and lower thermal conductivity of fuel raise the fuel temperature. Thus, in the fuel pin of low LHR or small Gw_0 and/or high initial density, the position of region b–c is beyond boundary A, and the rim structure is formed in both the lower and middle regions. On the other hand, the position of region b–c drops down below boundary A in the fuel pin of high LHR or large Gw_0 and/or low fuel density, also JOG is formed in the lower region. The LHR is low in region a–b where only the rim structure is observed with the large fuel swelling and small gap width, and thus the burn-up does not attain a high value.

5. Summary

The fuel-to-cladding gap widths were measured in a large number of FBR MOX fuel pins irradiated to high burn-up as a function of burn-up. By the optical microscope measurements showed when the burn-up increased progressively, the gap widths decreased due

to the fuel swelling up to about ~ 30 GWd/t. Beyond this burn-up, the dependence of gap width on the burn-up was closely related to the formations of JOG in the gap and rim structure in the fuel matrix. In the axial region of low fuel temperature, the gap width decreased due to the increase of fuel swelling resulting from the accumulation of fission products in the fuel matrix, and the rim structure appeared on its periphery. On the other hand, in the axial region of high fuel temperature, the volatile fission products were released with fission gases from the fuel matrix, and then accumulated and formed JOG in the gap. As a result, the fuel swelling decreased and gap width increased with the increase of burn-up.

Acknowledgements

The authors gratefully acknowledge very helpful discussions with Dr Hiroataka Furuya (Professor Emeritus, Kyusyu University). They also wish to thank Messers Kosuke Tanaka, Yukihiro Osato, Yasuhiro Onuma and Sadayoshi Nukaga of the fuel monitoring section for their technical support in the examinations and helpful discussions on the results.

References

- [1] A.M. Ross, R.L. Stout, AECL-1552, 1962.
- [2] I. Johnson, C.E. Johnson, IAEA-SM-190/43, 1975, p. 99.
- [3] H. Furuya, S. Ukai, S. Shikakura, Y. Tsuchiuchi, K. Idemitsu, J. Nucl. Mater. 201 (1993) 46.
- [4] M. Tourasse, M. Boidron, B. Pasquet, J. Nucl. Mater. 188 (1992) 49.
- [5] C.T. Walker, T. Kameyama, S. Kitajima, M. Kinoshita, J. Nucl. Mater. 188 (1992) 73.
- [6] J.-C. Melis, J.-P. Piron, L. Roche, J. Nucl. Mater. 204 (1993) 188.
- [7] J.-C. Melis, H. Plitz, R. Thetford, J. Nucl. Mater. 204 (1993) 212.
- [8] T. Ishi, T. Mizuno, J. Nucl. Mater. 231 (1996) 242.
- [9] M. Naganuma, K. Maeda, N. Nakae, J. Rouault, J. Noirot, G. Crittenden, C. Brown, in: Proceedings of 6th International Conference on Nuclear Engineering (ICONE-6), San Diego, USA, ICONE-6257, 1998.